Polish J. Chem., **76**, 607–618 (2002)

Electrochemical Behavior of Pt - Au Alloys

by K. Kuśmierczyk[1], M. Łukaszewski[1], Z. Rogulski[1,2], H. Siwek[1,2], J. Kotowski[1] and A. Czerwiński[1,2*]

[1]*Department of Chemistry, Warsaw University, Pasteura 1, 02-093 Warsaw, Poland*
[2]*Industrial Chemistry Research Institute, Rydygiera 8, 01-793 Warsaw, Poland*

(Received June 5th, 2001; revised manuscript December 12th, 2001)

The electrochemical behavior of the Pt - Au alloys in the whole composition range has been studied by cyclic voltammetry. The alloys were prepared by electrochemical deposition and the bulk compositions were determined by EDAX analysis. The surface areas of the electrodes were calculated from charges needed for oxidation of hydrogen adsorbed on platinum and reduction of gold or platinum oxide monolayer. These data were used for the estimation of the surface composition. The results were compared with data obtained from double layer capacity measurements. The surface area and platinum concentration on the surface, calculated from charges needed for platinum and gold oxides reduction, are overestimated, because the charge needed for platinum oxide reduction corresponds to more than a one monolayer.

Key words: alloys, Pt - Au alloys, surface estimation

The electrochemical properties of noble metals and their alloys are still subjects of modern research. This can be attributed to search for new materials for electrocatalysis, electrosynthesis and, in particular, for fuel cell applications. The knowledge of electrochemical behavior allows a better understanding of the surface processes occurring on the electrode surface during electroanalysis. Metals of group 10 – Ni, Pd, Pt – possess the highest catalytic activity in hydrogenation reactions. The metals of neighbouring group – Cu, Ag, Au – are much less active in the same reactions.

Pt - Au alloy can be considered as a model system to study the mechanism of hydrogen adsorption on transition metals, because the ability of metals to adsorb hydrogen is closely linked to the electronic structure of their d-band. The valence d-orbitals of gold are filled, whereas platinum's are not. Therefore, varying the content of gold in the Pt - Au alloy we can obtain a metal substrate with a controlled d-band occupation. Lapteva *et al*. [1], studying Pt - Au alloys, attempted to explain the differences in adsorption properties of metals by their electronic structure. These studies were further carried on [2–5]. It was shown that there is no simple correlation between the number of vacancies in the d-band and hydrogen adsorption properties of the alloy or metal. Alloys with both very small and very large gold content have properties of a

*Corresponding author: e-mail aczerw@chem.uw.edu.pl

single phase (homogeneous alloys). The rest of the alloys are two-phase systems, containing a platinum-rich α_1 phase and a gold-rich α_2 phase. The α_1 phase has electrochemical properties almost identical with those of pure platinum and the α_2 phase acts like pure gold. From the X-ray analysis of the heterogeneous alloys [6] it was obtained that α_1 consists of 85% Pt and 15% Au, while α_2 consists of 25% Pt and 75% Au. The above conclusions are summarized on the Pt - Au phase diagram [7]. Woods [8] has studied the electrochemical behavior of Pt - Au alloys deposited electrochemically on platinum foil. The change of the electrocatalytic properties of the alloy electrode was studied for the acetate oxidation reaction. Lamy *et al*. studied the electrochemical behavior of Pt - Au alloys, modified by underpotential deposition of Pb adatoms [9], and in the presence of 2,2′-dipyridine complexes of ruthenium(II) and rhodium(III) and 2,2′-dipyridine itself [10]. These compounds were chosen as models of the bifunctional catalysts for water decomposition.

In most cases the Pt - Au alloys studied were prepared by co-electrodeposition of both metals on polycrystalline platinum [8–10], by volume melting of the metals [1–6,11] or by underpotential deposition of gold on platinum [12]. The results presented in this paper were obtained for the composition range of Pt and Au, in which Pt - Au alloys exhibit heterogeneous behavior. We also present the results for platinum – gold alloys before and after cycling in the full potential range for platinum and gold (0.06–1.57 V), *i.e*. between hydrogen evolution and surface oxides generation.

EXPERIMENTAL

The experiments were performed in 0.5 mol dm^{-3} H_2SO_4 solutions at room temperature. The solutions were deoxygenated by an argon stream for 15 min. A platinum gauze and an SSE (a sulfuric electrode saturated with K_2SO_4) were used as the auxiliary and the reference electrodes, respectively. All potentials presented are referred to the RHE. Solutions were prepared on triply distilled water using analytical grade reagents. The Pt - Au alloys were deposited on a gold wire at ambient temperature with a current density from 0.2 to 8 A dm^{-2} from a bath containing $HAuCl_4$ and H_2PtCl_6 in various concentrations in concentrated HCl [8–10,13]. The composition of the alloys was altered in a wide range by employing different electrolyte compositions and electrolysis parameters. The alloys obtained were kept 2–3 days in an argon atmosphere for ageing. The composition of the bulk of the alloy was obtained from the EDAX analysis (Röntec M1 analyzer coupled with LEO 435VP scanning electron microscope). The surface composition of the alloys was analyzed by electrochemical methods described in the literature for pure gold, platinum and alloy electrodes [8–11,14–18]. The results obtained with all methods have been compared. For comparison, pure (99.99%) platinum and gold wires of diameter 0.5 mm were also employed.

RESULTS AND DISCUSSION

After electrodeposition of the Pt - Au alloy, the electrode was cycled continuously from 0.06 V to 1.57 V at 0.5 V s^{-1} in 0.5 mol dm^{-3} H_2SO_4.

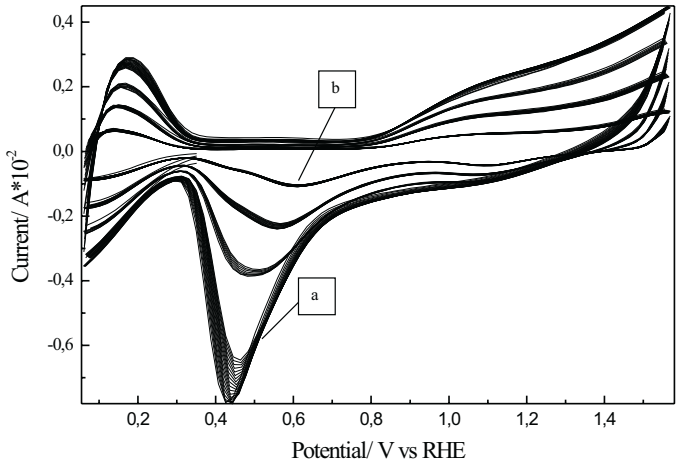

Figure 1. Voltammograms of freshly deposited Pt - Au alloy in 0.5 mol dm^{-3} H_2SO_4 recorded during cycling between 0.06 V and 1.57 V at scan rate 0.5 V s^{-1}. 1st scan (a) and 850th scan (b).

Figure 1 shows cyclic voltammograms of freshly deposited Pt - Au alloy (51.5% at Pt) recorded in 0.5 mol dm^{-3} H_2SO_4 with a scan rate of 0.5 V s^{-1}. It gives an illustration of the surface rearrangement of the alloy after long term electrochemical treatment (*ca*. 850 scans). Initially overlapping reduction signals and broad oxidation peaks for freshly prepared alloy gradually separate during cycling into signals typical for polycrystalline platinum and gold. The decrease of currents during electrode cycling gives also evidence for smoothening of the surface of the alloy during cycling.

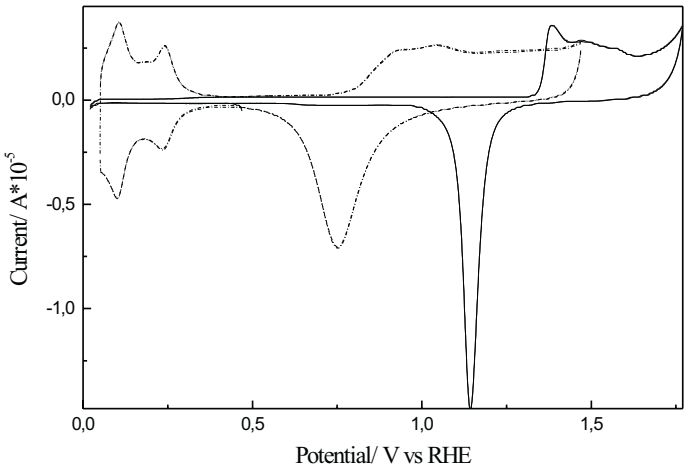

Figure 2. Superposition of voltammograms for pure polycrystalline gold (solid line) and platinum (dotted line) in 0.5 mol dm^{-3} H_2SO_4, scan rate 0.025 V s^{-1}.

The peaks are placed at potentials identical or very close to the potentials of peaks recorded for the pure metals. This is an evidence for the existence of two surface phases [14]. In Figure 2 there is a superposition of voltammograms for pure polycrystalline gold and platinum in 0.5 mol dm^{-3} H_2SO_4 recorded at 0.025 V s^{-1}.

The reorganization of the surface is also illustrated on electron microscope images taken before and after electrochemical treatment (Fig. 3). A significant change of the particle size after cycling strongly supports the conclusion on the smoothing of the electrode surface during electrochemical pretreatment.

(a)

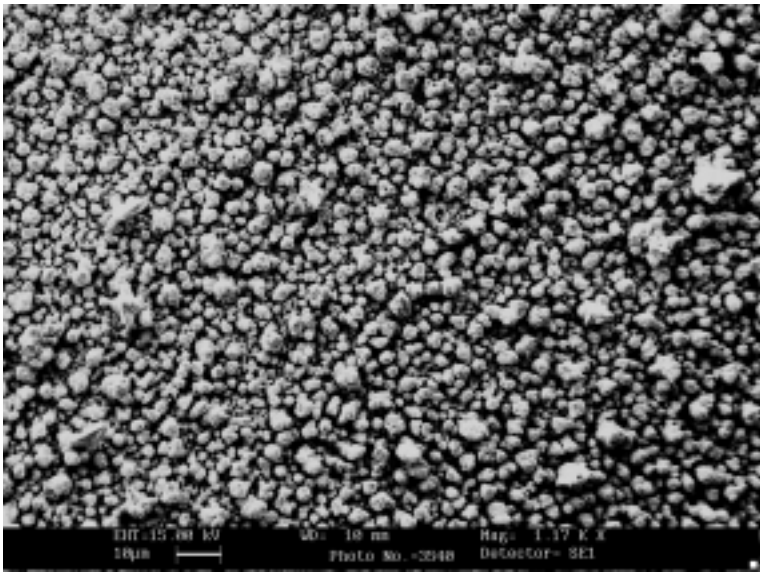

(b)

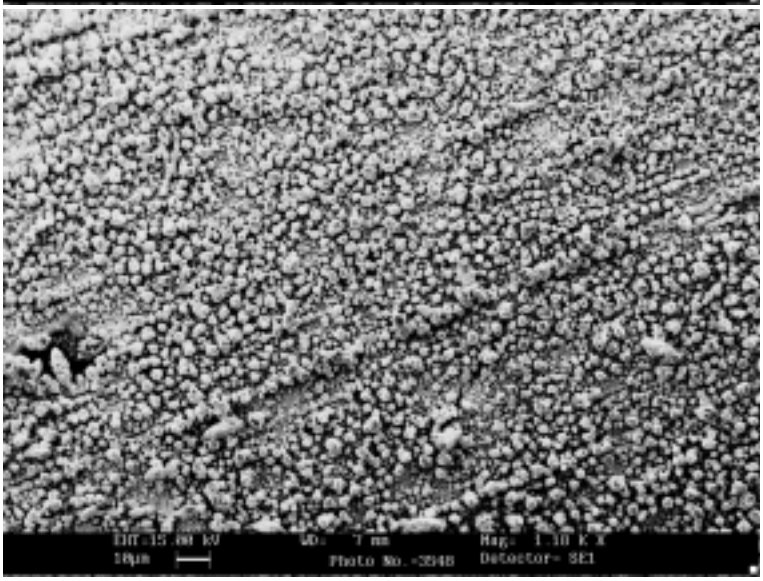

Figure 3. Electron microscope images of the alloy's surface: before (a) and after (b) electrochemical treatment (long cycling between 0.06 V and 1.57 V, scan rate 0.5 V s^{-1}).

Figure 4 presents typical I - E curves recorded for a heterogeneous Pt - Au alloy in 0.5 mol dm^{-3} H_2SO_4 with various scan rates (alloy after electrochemical treatment).

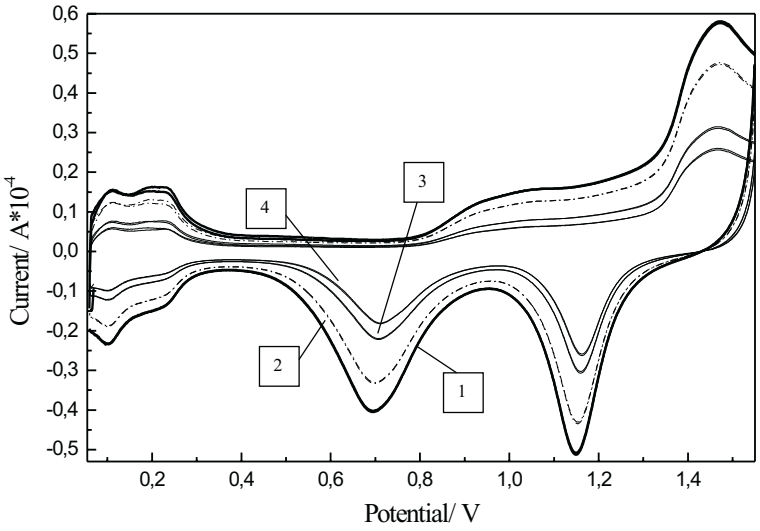

Figure 4. Voltammograms of Pt - Au alloy in 0.5 mol dm^{-3} H_2SO_4, scan rate 0.050 V s^{-1} (1), 0.040 V s^{-1} (2), 0.025 V s^{-1} (3), 0.020 V s^{-1} (4).

The curves' shape is basically the same as the one obtained for volume melted alloys of Pt and Au. The I - E curve for the alloy is a superposition of the curves for the pure metals. There are two regions of Pt - Au alloy electrooxidation, the first due to Pt oxide and the second to the Au oxide formation. On the cathodic scan there are respectively two reduction peaks, related to reduction of oxides formed during the anodic scan. One can also distinguish the hydrogen adsorption and desorption signals, due to the presence of platinum. Gold in this alloy is inactive in these processes. The oxide reduction peaks are well separated. It was established that increasing the gold content in the alloy from 0 to 90% results in a shift of the platinum oxide reduction peak by 0.055–0.060 V in the cathodic direction. Correspondingly, increasing the platinum content from 0 to 95% causes the gold oxide reduction peak to move 0.015–0.030 V in the anodic direction. The shift is most pronounced for homogeneous alloys, *i.e.* at 0–10% gold content. Nevertheless, such small potential changes cannot be correlated with the surface composition of the alloy [6]. Due to the above considerations, hydrogen adsorption for heterogeneous Pt - Au alloys should be limited by the amount of the platinum-rich α_1 phase. The shape of the hydrogen desorption peaks is characteristic of Pt - Au alloys. It was found [2] that at least two almost equal peaks, observed for the polycrystalline platinum electrode in acidic media, attributed to weaker and stronger adsorbed hydrogen, are also observed for alloys with Au content up to 30%. When the gold content is above 30%, the hydrogen desorption signal becomes broad.

The surface composition changes during repeated potential cycling, because of easier platinum dissolution with respect to gold. It was established that this change is bigger when the anodic vertex potential is more positive. Figure 5a presents the modification of the surface of the alloy upon cycling between 0.06 V and 1.77 V in 0.5 mol dm^{-3} H_2SO_4 with the scan rate of 0.5 V s^{-1}. In subsequent cycles the signals related to the α_1 phase increase, whereas those related to the α_2 phase decrease.

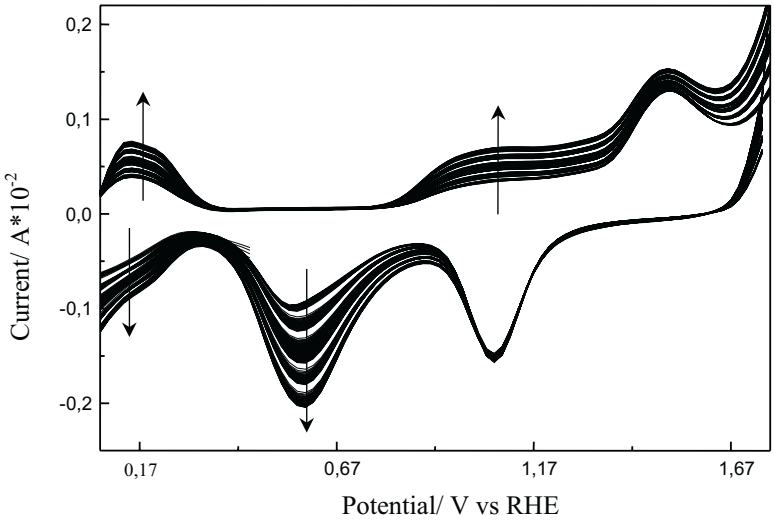

Figure 5a. Cyclic voltammograms of the Pt - Au alloy recorded during cycling between 0.06 V and 1.77 V in 0.5 mol dm^{-3} H_2SO_4, scan rate 0.5 V s^{-1}.

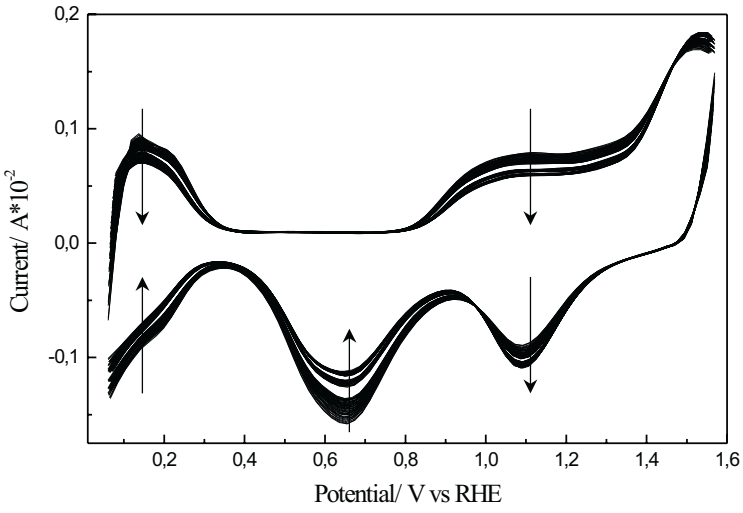

Figure 5b. Cyclic voltammograms of the Pt - Au alloy recorded during cycling between 0.06 V and 1.57 V in 0.5 mol dm^{-3} H_2SO_4 after cycling between 0.06 V and 1.77 V, scan rate 0.5 V s^{-1}.

Platinum atoms, taking part in the process of surface oxide formation, can either return to their original place or become adatoms in another place or even leave to the solution. The platinum ions from solution can discharge on the electrode to form adatoms. If a platinum atom leaves the electrode, exposing another platinum atom underneath and then deposits itself on the gold part of the surface, the platinum surface content increases. The latter process should increase the electrode roughness [18]. It is interesting to note that the increase of roughness should be observed mainly on the "platinum" part of the electrode. The "gold" part is more stable. Such a roughening is observed when the electrode is cycled in a wide range of potentials, which is in support for the above interpretation of increasing surface platinum content upon cycling. The effect of roughening of the alloy's surface, observed during electrode polarization between 0.06–1.77 V, is contrary to the smoothening observed after the alloy is cycled in the range of potentials 0.06–1.57 V (Figs. 1 and 3). The modified surface is not stable and during cycling in a narrower potential window the electrode returns to its favored initial state. Figure 5a presents the behavior of the Pt - Au alloy during electrode scanning in a wide potential range (0.06 V–1.77 V) and the same electrode's behavior after changing the high vertex potential to 1.57 V (Fig. 5b).

One of the main tasks of our work was to compare and establish the right ways of real surface and composition determination for the Pt - Au electrode. Both these parameters can be estimated from charges needed for reduction of surface oxides of platinum and gold. The main problem with this method is the great difference in potential ranges of surface oxide formation for Pt and Au, which starts at 0.8 V for Pt and 1.35 V for Au [11,14]. This means that at the completion of surface oxide formation on gold platinum is already fully oxidized and oxygen evolution probably takes place. At high anodic potentials the structure of platinum oxide is also different than that at less positive potentials [14]. Both facts can be the source of a positive error in the estimation of real area and surface concentration of platinum atoms. This error can be avoided by measurement of the charge needed for surface oxide reduction before gold (phase α_2) is fully covered with the oxide monolayer, *i.e.* after attaining the potential at which only platinum (phase α_1), but not gold, is fully covered by surface oxide. Breiter [3] and Woods [8,11] used the value 300 $\mu C\ cm^{-2}$ for the estimation of the area of α_2 from the cathodic oxide reduction peak, due to the α_2 phase (mainly gold), after polarization of the alloy electrode to 1.5 V. The surface covered with platinum particles was found from the charge needed for adsorbed hydrogen oxidation (on gold there is practically no hydrogen sorption). When using the full range of potentials (0.06–1.57 V), *i.e.* reaching a full coverage of the gold phase (α_2) with surface oxide, reliable results can be obtained if the platinum atoms concentration is calculated from the amount of hydrogen adsorbed on the Pt - Au electrode and at the same time gold is determined from the respective oxide monolayer reduction.

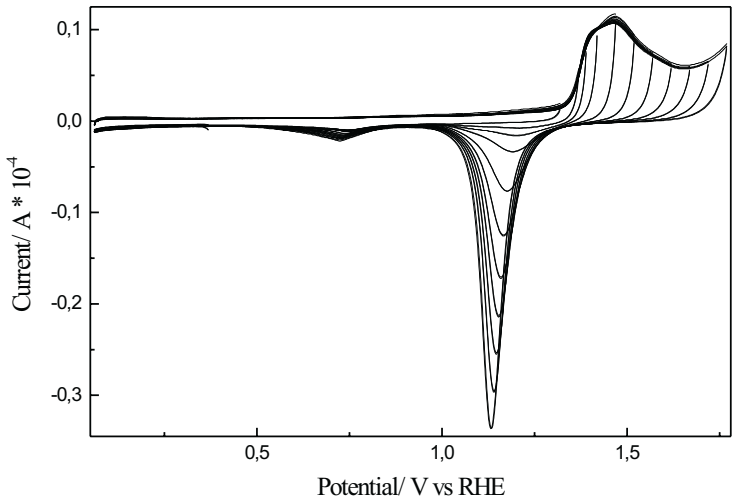

Figure 6a. Effect of the anodic limit of a potential sweep on the voltammograms of the heterogeneous Pt - Au alloy in 0.5 mol dm^{-3} H_2SO_4.

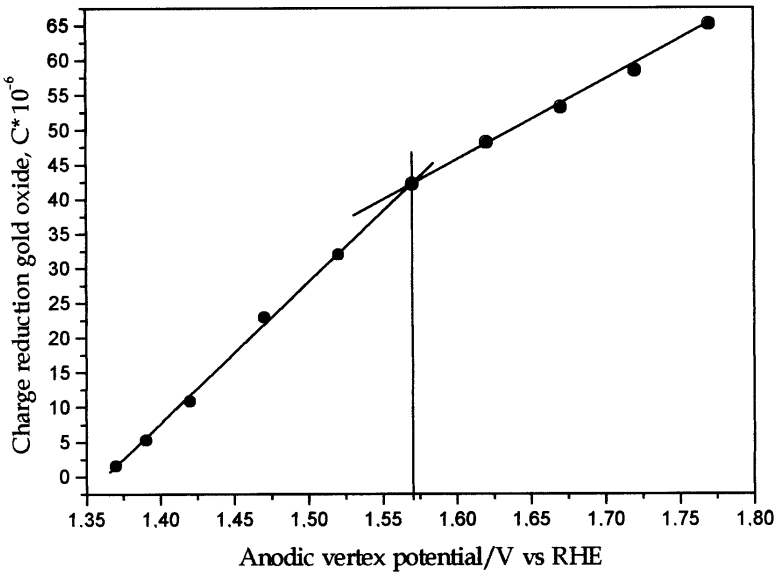

Figure 6b. Depedence of the gold oxide reduction charge on the anodic vertex potential for the Pt - Au alloy, scan rate 0.04 V s^{-1}.

Figure 6a presents cyclic voltammograms of the Pt - Au alloy (16% at Pt, scan rate 0.040 V s^{-1}) with different anodic vertex potentials. From the relationship between the gold oxide reduction charge and the anodic vertex potential (Fig. 6b) it follows that the monolayer of oxide formation is indeed completed at 1.57 V (the curve has a typical bend) [19]. For scan rates in the range 0.020–0.050 V s^{-1}, employed in our experiments, this potential is practically constant. From the gold oxide monolayer reduction charge, obtained for the Pt - Au surface, one can calculate the real area occupied by gold assuming that it takes 400 μC to reduce the oxide on 1 cm^2 of the electrode, *i.e.* the same value as for the polycrystalline gold electrode [14,16,19]. It differs from the value used by Woods [8] for Pt - Au area estimation after the electrode was polarized to 1.5 V. The amount of platinum (α_1 phase) on the surface was estimated from the hydrogen desorption charge, assuming that 210 μC corresponds to 1 cm^2 (the charge was calculated at a 0.77 coverage of the electrode by hydrogen to the current minimum that follows the second platinum cathodic hydrogen peak) [14]. When is not possible to establish the real electrode area from the well known surface processes (like hydrogen or oxygen monolayers formation/removal), the region of potentials, which is free from faradaic processes under linear potential sweep conditions, can be used. There, the double layer charging current is proportional to the differential capacity of the electrode. Figure 7 shows double layer charging curves for the Pt - Au alloy (58.1% at Pt) in 0.5 mol dm^{-3} H_2SO_4 in the potential range 0.37–0.67 V. The double layer capacity is calculated from the slope of the relationship between the

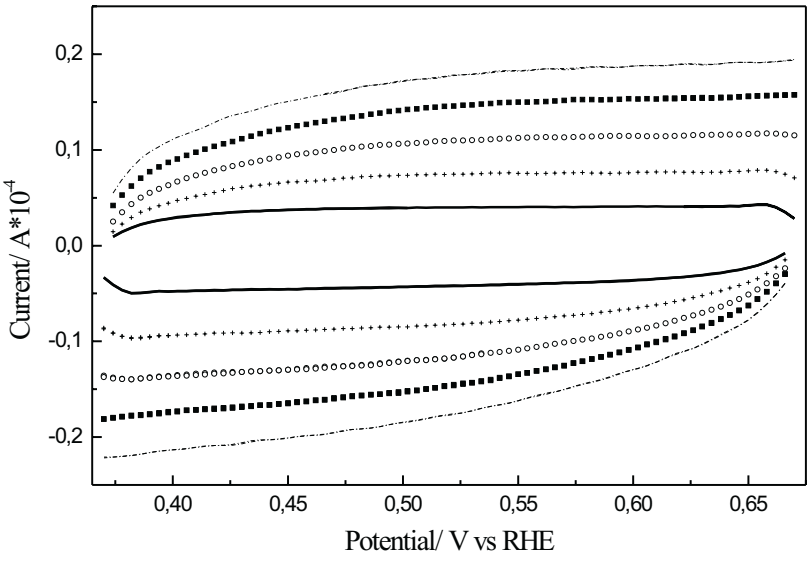

Figure 7. Double layer charging curves for the Pt - Au alloy in 0.5 mol dm^{-3} H_2SO_4, potential window 0.37–0.67 V, scan rate 0.5 V s^{-1} (·-·-·-·), 0.4 V s^{-1} (■■■), 0.3 V s^{-1} (ooo), 0.2 V s^{-1} (+ + +), 0.1 V s^{-1} (—).

double layer charging current at a given potential and the scan rate. The dependence was linear for all alloys studied and the correlation coefficients were in the range 0.90–0.98. From the capacity we can calculate the area of the electrode, assuming after [20], that the capacity of 1 cm^2 of pure platinum and gold equals 28 μF. This method gives good results in the absence of electroactive impurities in solution. Table 1 summarizes the real surface area and the surface composition for the same alloy estimated using the above methods. The alloy electrodes were cycled between 0.06 V to 1.57 V. The calculations were based on a voltammogram recorded after 850 scans. From charges needed for gold and platinum surface oxides reduction and hydrogen deposition on platinum, we calculated both the surface area and the surface composition. For comparison we have demonstrated also the data obtained from the double layer capacity. One can see that there is a difference between the real surface area estimated from charges needed for oxides reduction on gold and hydrogen oxidation on platinum (method I) in comparison with the real surface area estimated from charges needed for oxides reduction on platinum and hydrogen oxidation on platinum (method II). In spite of different surface compositions of the Pt - Au alloys, the difference between the two methods is rather constant and has an average value of about 10%. From our experimental data the charge needed for platinum oxide reduction after the pure platinum electrode polarization to 1.57 V (at this potential the Pt - Au electrode is covered with a monolayer of gold oxide) is *ca*.12% higher than the charge needed for platinum oxide monolayer reduction. It partially supports our results obtained with the Pt - Au alloys, but, at this moment, there is no answer why this difference is rather constant in the whole range of surface composition. It should increase with platinum concentration. Probably, it is one of the effects of interaction between Pt and Au atoms in the lattice. Both methods gave also information on the surface composition of the Pt - Au alloys. It is difficult to state at which anodic vertex potential the platinum oxide monolayer is completely formed. On the plot of the platinum oxide reduction charge *vs* the anodic vertex potential there is no characteristic bend, which can be found for gold. The platinum oxide reduction signal, therefore, can be used for surface estimation in the case when the hydrogen signal is not well developed, *i.e*. when the gold content is above 30% [2,5]. The true area of the Pt - Au electrode can be also judged from the double layer capacity. Those results are also included in Table 1. The method was used for real surface estimation of silver and copper electrodes [21,22] and Pt - Au alloys [17]. It has to be noted that in the same conditions this method was working only for the alloy studied. The results, obtained under the same laboratory conditions for the real surface estimates of pure gold and platinum, using the same capacity, which was taken for the alloy, are higher than those found from surface reactions (*i.e*. hydrogen or surface oxide adsorption/desorption).

Table 1. The real surface area of electrode and composition of alloys obtained with different methods.

Composition of alloy after electrode preparation by CV sweeps in potential range 0.06–1.57 V (Pt % at)		S_{Pt} (cm^2)		S_{Au} (cm^2) calculated from reduction charge of gold oxide monolayer AuO	S_{real} (cm^2)		Difference in calculated area with both methods (%)	S_{real} (cm^2) calculated from double layer capacity
in the bulk (EDAX data)	on the surface (calculated by method I)	calculated from oxidation charge of hydrogen adsorbed on platinum $S_{Pt}(H)$ (a)	calculated from reduction charge of surface platinum oxides $S_{Pt}(O)$ polarization potential range 0.06–1.57 V (b)	(c)	**I** calculated as sum $S_{Pt}(H) + S_{AuO}$ **(a + c)**	**II** calculated as sum $S_{Pt}(O) + S_{AuO}$ **(b + c)**		
32.6	13.1	0.02 ± 0.01	0.05 ± 0.003	0.11 ± 0.01	**0.13 ± 0.02**	**0.16 ± 0.04**	18.8	**0.14 ± 0.01**
40.0	23.3	0.26 ± 0.01	0.37 ± 0.02	0.86 ± 0.04	**1.12 ± 0.05**	**1.23 ± 0.06**	8.9	**1.12 ± 0.01**
48.2	29.9	0.32 ± 0.02	0.45 ± 0.02	0.75 ± 0.04	**1.07 ± 0.06**	**1.20 ± 0.06**	10.8	**1.08 ± 0.01**
49.9	36.6	0.15 ± 0.01	0.26 ± 0.01	0.26 ± 0.01	**0.41 ± 0.02**	**0.52 ± 0.02**	21.2	**0.45 ± 0.05**
51.2	37.5	0.72 ± 0.04	0.78 ± 0.04	0.43 ± 0.02	**1.15 ± 0.06**	**1.21 ± 0.06**	5.0	**1.18 ± 0.01**
58.3	42.7	1.03 ± 0.05	1.12 ± 0.06	1.50 ± 0.08	**2.53 ± 0.13**	**2.62 ± 0.14**	3.4	**2.25 ± 0.02**
60.1	54.1	0.38 ± 0.02	0.45 ± 0.02	0.31 ± 0.02	**0.69 ± 0.04**	**0.76 ± 0.04**	9.2	**0.70 ± 0.07**
70.1	58.3	0.24 ± 0.01	0.27 ± 0.01	0.17 ± 0.01	**0.41 ± 0.02**	**0.44 ± 0.02**	6.8	**0.42 ± 0.04**
82.1	60.9	0.37 ± 0.02	0.41 ± 0.02	0.20 ± 0.01	**0.57 ± 0.03**	**0.61 ± 0.03**	6.6	**0.55 ± 0.06**
89.3	70.1	0.40 ± 0.02	0.45 ± 0.02	0.17 ± 0.01	**0.57 ± 0.03**	**0.62 ± 0.03**	8.1	**0.56 ± 0.06**

Acknowledgment

This work was financially supported by The University of Warsaw (120-501/68-BW-1483/17/2000).

REFERENCES

1. Lapteva K.A., Borissova T.I. and Slinko M.G., *Zhur. Fiz. Khim*., **30**, 61 (1956).
2. Breiter M.W., *J. Electroanal. Chem*., **8**, 230 (1964).
3. Breiter M.W., *J. Phys. Chem*., **69**, 901 (1965).
4. Breiter M.W., *Electrochim. Acta*, **10**, 543 (1965).
5. Breiter M.W., *Trans. Farad. Soc*., **61**, 749 (1965).
6. Radjuszkina K.A., Bursztein R.H., Tarasewicz M.R. and Kuprina W.W., *Elektrokhimiya*, **6**, 237 (1970).
7. Łoskiewicz W. and Orman M., *Equilibria in Binary Metallic Alloys*, PWN, Warszawa (in Polish) (1956).
8. Woods R., *Electrochim. Acta*, **14**, 553 (1969).
9. Beden B., Kadirgan F., Kahyaogolu A. and Lamy C., *J. Electroanal. Chem*., **135**, 329 (1982).
10. Enea O. and Lamy C., *Electrochim. Acta*, **28**, 1741 (1983).
11. Woods R., *Electrochim. Acta*, **16**, 655 (1971).
12. Furuya N. and Motoo S., *J. Electroanal. Chem*., **88**, 151 (1978).
13. Harrison J.A. and Thompson J., *Electrochim. Acta*, **18**, 829 (1973).
14. Woods R., in: *Electroanalytical Chemistry* (Bard A.J., Ed.) Vol. 9. Marcel Dekker, NY (1976).
15. Trasatti S. and Petrii O.A., *Pure Appl. Chem*., **63**, 711 (1991).
16. Friedrich K.A., Henglein F., Stimming U. and Unkauf W., *Electrochim. Acta*, **45**, 3283 (2000).
17. Conway B.E., Angerstein-Kozłowska H. and Czartoryska G., *Z. Phys. Chem*., **112**, 195 (1978).
18. Rach E. and Heitbaum J., *Electrochim. Acta*, **32**, 1173 (1987).
19. Brummer S.B. and Makrides A.C., *J. Electrochem. Soc*., **111**, 1122 (1964).
20. Waszczuk P., Zelenay P. and Sobkowski J., *Electrochim. Acta*, **40**, 1717 (1995).
21. Smoliński S., Zelenay P. and Sobkowski J., *J. Electroanal. Chem*., **442**, 41 (1998).
22. Smoliński S. and Sobkowski J., *J. Electroanal. Chem*., **463**, 1 (1999).